

## CRUDE OIL FOULING IN A PILOT-SCALE PARALLEL TUBE APPARATUS

B. D. Crittenden, S. T. Kolaczowski, T. Takemoto and D. Z. Phillips

Department of Chemical Engineering, University of Bath, Bath, UK, BA2 7AY, E-mail: B.D.Crittenden@bath.ac.uk

### ABSTRACT

Maya crude oil fouling reveals a seemingly straightforward dependency of initial fouling rate on surface temperature but a maximum is found in the initial fouling rate – velocity relationship which mirrors that found in a model chemical system of styrene polymerization. The linear dependency of the logarithm of the pre-exponential factor on apparent activation energy for the crude oil is also found in the styrene system. The apparent activation energy for the crude oil ranged from 26.4 kJ/mol at 1.0 m/s to 245 kJ/mol at 4.0 m/s. Such strong dependencies of apparent activation energy on velocity, even at high velocity, are consistent with Epstein's mass transfer-reaction-attachment model. Surface temperatures at which the fouling rate becomes velocity-independent are 274°C and 77°C for Maya crude oil and styrene, respectively. For surface temperatures in excess of this isokinetic temperature, an increase in velocity would lead to an increase in the rate of fouling.

### INTRODUCTION

Several types of laboratory apparatus have been used to study crude oil fouling. Each has its limitations with none representing the once-through shell-and-tube configuration used in oil refineries. Consequently, there will always be doubts over the applicability of laboratory data to the refinery situation, doubts which are compounded by the challenges of interpreting refinery data (Takemoto et al., 1999). The ideal method of HTRI's Crude Oil Fouling Task Force (COFTF) would be to monitor fouling inside a 19-25 mm tube (Bennett et al., 2006). Even so, COFTF's preferred design is of the annular type, comprising a flow loop with a cartridge heater sheathed with the metallurgy of interest and placed in an annular flow gap of 2-5 mm.

Tubular fouling apparatus have been heated by radiant heat transfer (Crittenden and Khater, 1987) and by electrical elements wound around the outside of the tube (Crittenden et al., 1987a). Principal advantages are that flow rates, turbulence structures, bulk temperatures, surface temperatures and heat fluxes typical of industrial practice can be used with the desired metallurgy. In addition, the effects of in-tube devices can be studied (Crittenden et al., 1993). Principal disadvantages are the continued recirculation of crude oil and the difficulty of gaining good access to the deposit unless the tube is sectioned after shut down. The fouling resistance  $R_f$  can be calculated from Eq. (1) (Crittenden et al., 1987a; Bennett et al., 2006).

$$R_f = \left( \frac{T_s - T_b}{q} \right)_t - \left( \frac{T_s - T_b}{q} \right)_{t=0} \quad (1)$$

Here,  $q$  is the heat flux and  $T_s$  and  $T_b$  are the local surface and bulk temperatures at time  $t$  and time zero, respectively. This equation avoids the need to calculate film heat transfer coefficients and all the errors associated with estimating their parameters. At constant bulk temperature and constant heat flux, Eq. (1) becomes:

$$R_f = \left( \frac{T_{st} - T_{so}}{q} \right) \quad (2)$$

Here,  $T_{st}$  and  $T_{so}$  are the surface temperatures at time  $t$  and zero, respectively. The instantaneous rate of fouling is now proportional to the instantaneous rate at which the surface temperature changes.

### EXPERIMENTAL

Concerns over the repeatability of fouling data in consecutive runs with the same crude oil charge led Takemoto (1993) to adopt the twin parallel tube, recirculation flow configuration described elsewhere (Crittenden et al., 1993) and shown in Fig. 1. Good reproducibility of fouling rates in the two parallel tubes in any given run were found, even though reproducibility from run to run was less certain. The challenge of ensuring comparability in local fouling rates in the two parallel tubes when HiTRAN inserts were used was also overcome (Crittenden et al., 1993).

The main items in the flow loop (Fig. 1) were a 0.105 m<sup>3</sup> heated reservoir (2 kW) and a Worthington Simpson 40/20 CMR 125 centrifugal feed pump fitted with a variable speed magnetic drive (Danfoss VLT 101). Flow rates to the two parallel test sections were individually controlled and monitored using KDG 9300 series flow meters. A by-pass, for circulating crude oil through the reservoir whilst it was being heated, contained two 1 kW "K-ring" heaters supplied by Watlow Ltd. The apparatus was pressurised and maintained automatically at 15 bar using a moveable piston which separated nitrogen gas from the crude oil. Free movement of the piston allowed the bulk pressure to remain constant as the test fluid expanded or contracted with temperature. The two horizontal tubular test sections comprised standard tubing (to A179 specification),

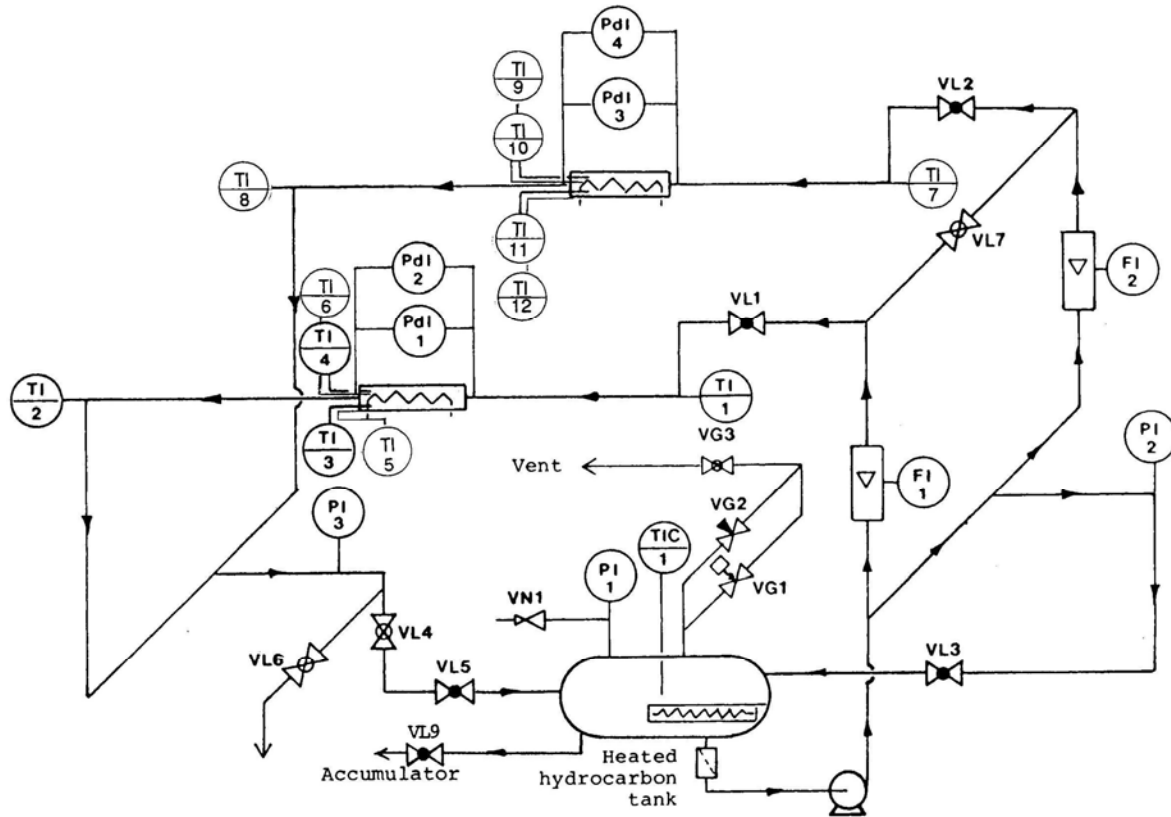


Fig. 1 Schematic of the pilot-scale parallel tube apparatus (Takemoto, 1993)

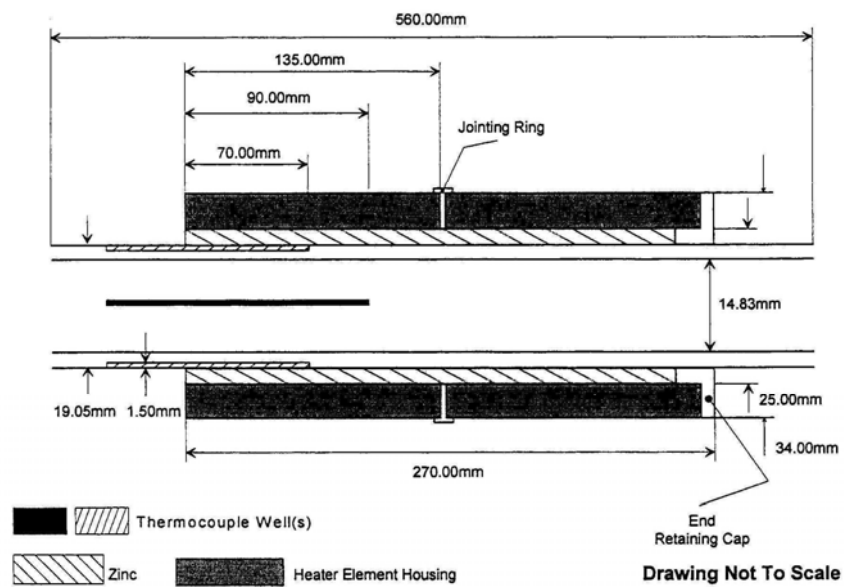


Fig. 2 Schematic of heated test section (Phillips, 1999)

of overall length 560 mm and with inside and outside diameters of 14.83 and 19.05 mm, respectively. Heat was provided by external electrical elements over a length of 270 mm, the power being controlled independently in each test section by a Variac transformer and monitored by a wattmeter (Tabor Electronics UDW 4501).

The original tube heater design (Takemoto, 1993) was found to be fragile and the revised design shown in Fig. 2 (Phillips, 1999) used two “K-ring” heaters (connected together with a jointing ring) housed within a rigid tube. Brass formed the inner surface to which the elements were attached, a stainless steel sheath protecting them from the environment. The revised design enabled heat fluxes up to 282 kW/m<sup>2</sup> to be used. The void in the heater assembly was filled with zinc, chosen because of its high thermal conductivity and low melting point of 419°C. Thus, near perfect filling of the voids with zinc could be achieved using the electrical heating elements to melt the metal so that it filled the void prior to allowing it to solidify.

As an enhancement to Takemoto’s design in Fig. 1, three surface thermocouples were placed in grooves on the tubing at 120° separation at each of two axial locations (not all shown in Fig. 2). When annular flow arrangements are used with a test section swaged onto a heater, regular calibration is needed to determine the contact resistance which can change due to repeated thermal expansions and contractions (Bennett et al., 2006). In contrast, in the zinc-filled tubular system the thermal resistances between the thermocouples and the inner surface of the exchanger tube always remain negligible. To demonstrate this advantage, the Wilson (1915) method was used with non-fouling Santotherm SP 50 (Phillips, 1999). No significant variations were found between the six thermocouple readings as fouling proceeded at constant heat flux. This is expected since the temperature change from one axial location to the other was small. Accordingly, the average of the six surface temperatures has been used in Eq. (2).

Maya crude oil was selected because it was expected to foul under pilot-scale conditions and because it contained a low percentage of light ends, thereby making it easier to handle in the laboratory (Phillips, 1999). The oil was not filtered. Typical properties (Energy Institute, 2004) are: 21.1 API gravity, vapour pressure in the range 6.2-6.7 psig, 0.55% gas w/w, 4.03% total wax w/w, -21°C pour point, calculated cloud point in the range 17-40°C, and viscosities of 161.5 and 54.80 mm<sup>2</sup>/s at 30°C and 50°C, respectively. Tanaka et al. (2001) determined that their sample of Maya crude oil contained 82.0 wt% carbon, 7.5% hydrogen, 7.1% sulphur, 1.3% nitrogen, 1.2% oxygen together with 390 ppm (by weight) nickel and 1800 ppm vanadium. In the current research, the physical properties of Maya crude oil were obtained from the American Petroleum Institute (API) Technical Data Book (1988). The Watson K value was

Table 1. Summary of Experimental Runs

Velocity m/s	Re	Initial (clean) surface temperature			
		250°C	265°C	270°C	280°C
0.5	3,600	√			√
0.8	5,800	√			√
1.0	7,300	√	√	√	√
1.5	11,000	√	√	√	√
2.0	14,500	√	√	√	√
3.0	21,800	√	√	√	√
3.6	26,200	√	√	√	√
4.0	29,000	√	√	√	√

determined to be 11.72. The fluid properties were assumed to remain constant from run to run.

## RESULTS

A series of 65 runs was carried out with a bulk temperature and pressure of 150°C and 15 barg, respectively. The ranges of principal variables are summarized in Table 1. The values of Re are calculated from properties at the bulk temperature. Visual inspection revealed that deposits seemed to accumulate only in the heated portions of the test sections. The deposits were relatively soft and appeared to have high free oil contents.

The test sections were cleaned after each run by brushing after the tubes were drained of oil. Deposit samples were collected after some runs. Residual oil was first allowed to drain from the tube by standing it vertically. Deposits were then carefully removed from inside the test section by repeated insertion and removal of a wire insert which maintained a close fit with the inner wall. Method ASTM D893-92 was used to analyse the crude and its deposits for its major fractions. Little variation in deposit composition with flowrate, or indeed with initial surface temperature, was found. The asphaltene content of Maya crude oil was found to be *c.* 10% (lower than the 24.9% w/w found by Tanaka et al. (2001) in their sample), whilst the average asphaltene content in the deposits was 18%. This suggests that asphaltenes pre-existing in the crude oil had been concentrated at the surface during the fouling process. The resin plus free oil content was about 80%, higher than might be expected, but this is almost certainly the result of removing significant quantities of free oil from within the tube when removing the deposits. The high percentage of these groups almost certainly means that the asphaltene content of the actual deposit would have been rather more than 18%. For much the same reason, the coke and ash content was found to be very low at around 1%, making ash analyses impractical.

Table 2. Onset of Fouling

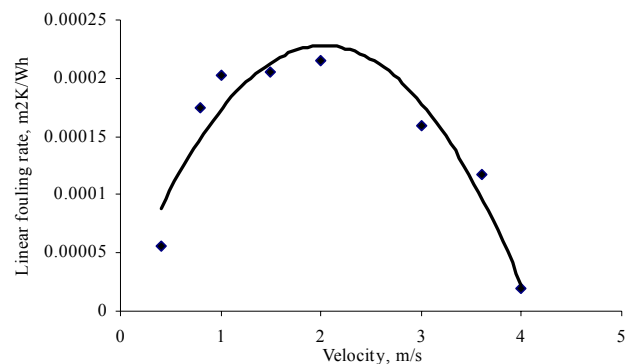
Test section	$T_{SO}$ (°C)	Average velocity (m/s)	Linear fouling rate $\times 10^4$ (m <sup>2</sup> K/Wh)
1	300	2.0	Very high
2	300	3.0	Very high
1	200	2.0	No fouling
2	200	0.5	No fouling
1	225	2.0	No fouling
2	225	0.5	No fouling
1	280	2.0	6.59
2	280	0.5	6.64
1	230	0.5	1.90
2	230	2.0	No fouling
1	200 → fouling onset	3.0	Fouling at 250°C
2	200 → fouling onset	2.0	Fouling at 240°C

Six initial pairs of runs were carried out to find the threshold temperature for the onset of fouling (Table 2). Surface temperatures of 300°C resulted in very high fouling rates at both velocities (2.0 and 3.0 m/s), to an extent that it was difficult to control the temperature precisely. Fouling had increased the surface temperature in the test sections to the 400°C safety cut off after only 15 minutes. Fouling was obtained at a surface temperature of 280°C, whilst at 230°C fouling was obtained at 0.5 m/s but not at 2.0 m/s. Fouling was not detected with initial surface temperatures of 200 and 225°C. For the final test, average velocities were set at 2.0 and 3.0 m/s and the power supplied to each test section adjusted to give initial surface temperatures of 200°C. No fouling occurred in the first 30 minutes. The power was then increased by 200 W for a further 30 minutes and the process of power increase continued stepwise until fouling became evident. These experiments revealed that at 2.0 m/s the threshold fouling temperature seemed to be about 240°C, whilst for 3.0 m/s it seemed to be about 250°C, these observations being consistent with the others shown in Table 2.

To gauge the strength of adhesion of deposits to the tube surface, the velocity in one of the test sections in the last test of Table 2 was increased from 2.0 to 3.0 m/s for a short period after fouling had commenced. The velocity was then returned to 2.0 m/s. This experiment seemed to show that the velocity increase had little effect on either the fouling resistance or the fouling rate once the velocity had been returned to the original value. This would suggest that at a bulk velocity of 2.0 m/s and surface temperature of 250°C, the fouling deposits were adhering strongly enough to the surface to be resistant to removal by a simple increase in fluid shear.

All subsequent experiments (Table 1) were carried out with a minimum initial surface temperature of 250°C to ensure that fouling occurred in both test sections. The first three fouling runs were carried out under identical conditions in both test sections ( $T_{SO} = 250^\circ\text{C}$ ;  $u = 2.0$  m/s). Reproducibility between the transient thermal data for the two parallel test sections was excellent but there was a marked difference between the data for the first run compared with that for the second and third runs. An asymptote seen in the two test sections for the first run must have been due to initial conditioning of the test section surfaces by the crude oil. The mechanism for this is uncertain but commentators suggest it is due to sulfiding of the metal surface when exposed to hot crude oils. In all subsequent runs, the fouling-time graph was more-or-less linear in shape, with no evidence of either induction periods or asymptotic fouling. Hence, all fouling rates obtained using data over the first five hours were considered to be initial rates. For all runs, the fluid velocity in one of the two test sections was set to be 2.0 m/s, this test section being used as the benchmark against which data in the other test section could be compared in the same run. In total, eight runs were carried out with  $u = 2.0$  m/s and  $T_{SO} = 250^\circ\text{C}$ , the average fouling rate being  $2.15 \times 10^{-4}$  m<sup>2</sup>K/Wh with a variation of less than  $\pm 10\%$ .

The average fouling rate for  $T_{SO} = 250^\circ\text{C}$  is shown as a function of velocity in Figure 3. There are some important features. Firstly, there is a maximum in the fouling rate as a function of velocity. This was observed in experiments with the model chemical system of styrene polymerization (Crittenden et al., 1987a). Secondly, the curve tends towards the origin as the velocity is reduced. This might perhaps be expected since as the velocity approaches zero, the fouling process would tend towards pure diffusion control. This tendency of the fouling rate to approach zero was not observed clearly in the styrene polymerization

Fig. 3 Linear fouling rate for  $T_{SO} = 250^\circ\text{C}$

study however. Thirdly, the fouling rate decreases significantly from its peak value as the velocity is increased from *c.* 2.0 m/s towards 4 m/s. This is encouraging since it is within this velocity range that refiners would normally operate the tube side of crude preheat exchangers.

The data of Fig. 3 have been normalized by dividing the fouling rate at the given velocity by that found in the test section operating at 2.0 m/s. The normalized fouling rate is plotted against the normalized velocity (actual velocity divided by 2.0 m/s) in Fig. 4. Reassuringly, this plot, which is made to eliminate variations that might arise from run to run, takes a shape which mimics closely that in Fig. 3. Had there been significant differences in the shapes of the curves in Figs. 3 and 4 then this would be indicative of poor reproducibility between the two test sections in the same run.

The effect of  $T_{SO}$  on the fouling rate for four surface temperatures is shown in the normalized plots of Fig. 5. These trends with surface temperature and velocity are mimicked by the styrene polymerization system (Crittenden et al., 1987a). For a given velocity, the fouling rate increases with surface temperature, as expected. A maximum in the fouling rate-velocity curve is seen for each of the four surface temperatures, the position of the maximum tending to shift towards a higher linear velocity as the surface temperature is increased. This might be expected as the relative balance between mass transfer effects and kinetic effects should shift towards mass transfer control as  $T_{SO}$  is increased (Crittenden et al., 1987a). The general Arrhenius expression is as follows:

$$\left. \frac{dR_f}{dt} \right|_{t=0} = A \exp(-E_A/RT_{SO}) \quad (3)$$

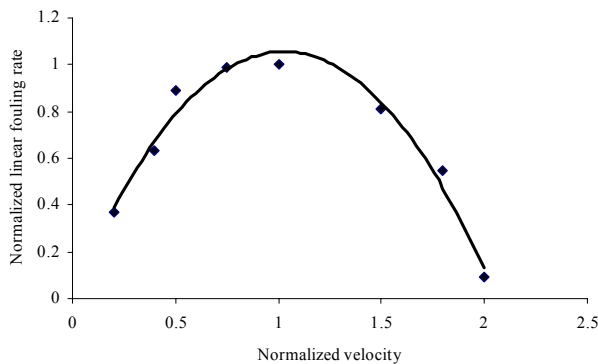


Fig. 4 Normalized linear fouling rate for  $T_{SO} = 250^\circ\text{C}$

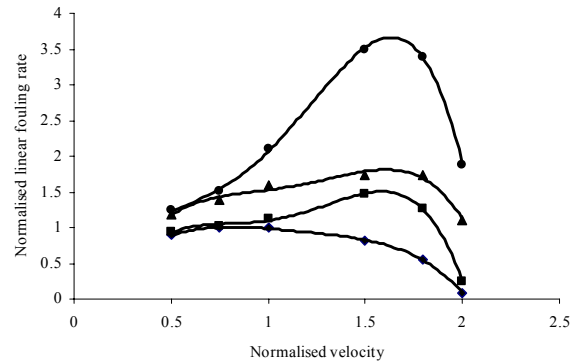


Fig. 5 Effect of surface temperature on normalized fouling rates, ( $\diamond$ ,  $250^\circ\text{C}$ ;  $\blacksquare$ ,  $265^\circ\text{C}$ ;  $\blacktriangle$ ,  $270^\circ\text{C}$ ;  $\bullet$ ,  $280^\circ\text{C}$ )

in which  $E_A$  would be the apparent activation energy for the fouling process. The strong influence of velocity (Fig. 5) means that it is not possible to evaluate the true activation energy,  $E$ , for the reaction aspects of the Maya crude oil fouling process. Apparent activation energies,  $E_A$ , can nevertheless be obtained by plotting the log of the fouling rate against the reciprocal of the absolute initial (clean) surface temperature,  $T_{SO}$ , for each velocity  $u$ .

An example Arrhenius plot for 3.6 m/s is shown in Fig. 6. Linearity of the plot was equally good for the other velocities studied with the Maya crude oil. Equally good Arrhenius plots were obtained for the styrene polymerization system as well (Crittenden et al., 1987a).

The variation of apparent activation energy with fluid velocity is shown in Fig. 7. At the lowest velocity, the low apparent activation energy indicates that the fouling process

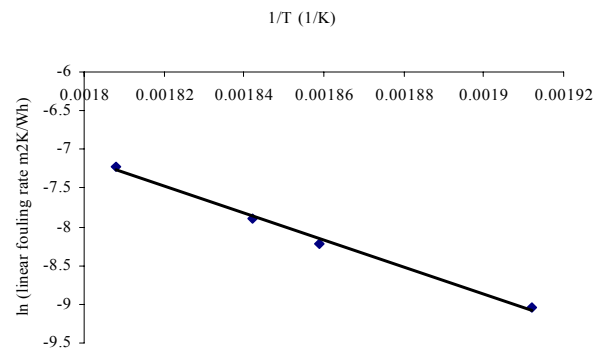


Fig. 6 Arrhenius plot for 3.6 m/s

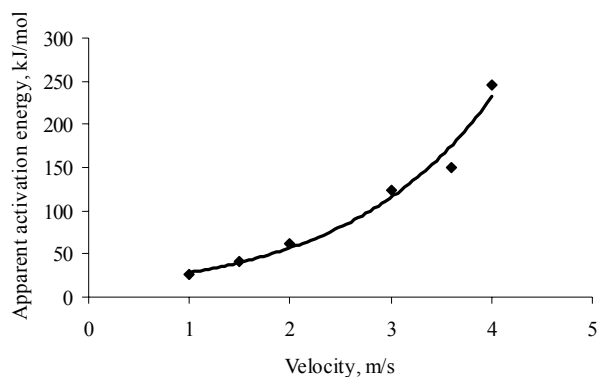


Fig. 7 Effect of velocity on apparent activation energy for Maya crude oil.

is dominated by physical phenomena. At the higher velocities, Fig. 7 shows that  $E_A$  remains a very strong function of velocity. Superficially, this might seem surprising since it ought, in principle, to be possible to increase the velocity to a point beyond which mass transfer effects become negligible such that the overall fouling process becomes solely kinetically controlled.

Of particular note, the trend of Fig. 7 for Maya crude oil is mimicked by a broadly similar trend for the styrene polymerization (Fig. 8) which has a lower apparent activation energy, most probably because styrene is able to polymerize quickly at low temperature. Even at high velocity when kinetics control might be expected, the effect

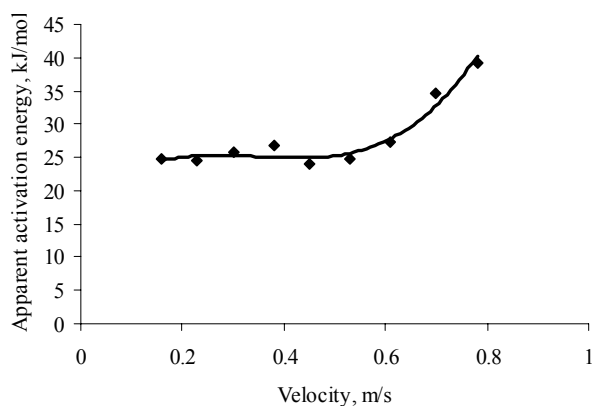


Fig. 8 Effect of velocity on apparent activation energy for styrene polymerization.

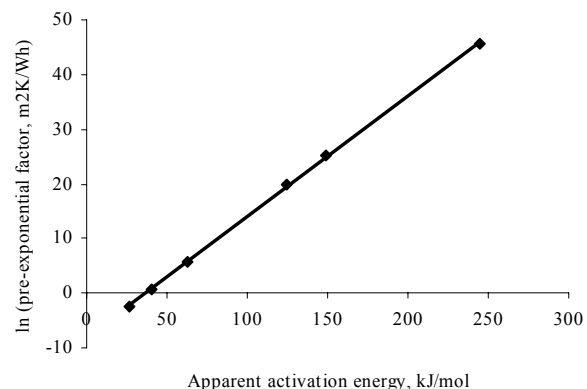


Fig. 9 Relationship between pre-exponential factor and apparent activation energy for Maya crude oil.

of velocity does not disappear in either fouling system. No attempt has been made to correlate apparent activation energies with other properties of the fluids.

Remarkably, the plot of the natural logarithm of the pre-exponential factor  $A$  against the apparent activation energy  $E_A$  is linear for Maya crude oil (Fig. 9). The gradient of the plot in Fig. 9 is 0.22 mol/kJ. Even more remarkably, an almost perfect linear relationship is observed with the styrene polymerization system as well (Fig. 10). The gradient of the plot in Fig. 10 is 0.34 mol/kJ. The value of these linear relationships between pre-exponential factors and apparent activation energies will be addressed later in the paper.

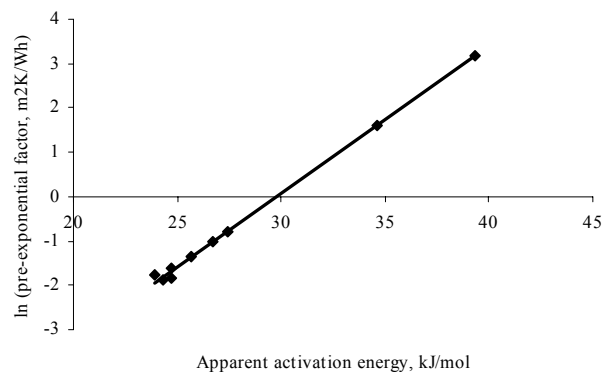


Fig. 10 Relationship between pre-exponential factor and apparent activation energy for styrene polymerization.

### TRANSFER, REACTION AND ATTACHMENT

Crittenden and Kolaczowski (1979) developed a general chemical reaction fouling model in which the kinetic aspects of the overall process were treated in series with the mass transfer aspects. The model was later developed to include a back-diffusion term in an attempt to account for the results obtained in the styrene polymerization system (Crittenden et al., 1987b). Epstein (1994) criticised this model because at time zero it is fundamentally difficult to justify a finite concentration of foulant at the wall which would be required for back-diffusion to occur. Accordingly, Epstein (1994) developed a model for the initial chemical reaction fouling at a heat transfer surface in which surface attachment, treated as a process in series with mass transfer, was assumed to vary directly with the residence time of the fluid at the surface. The "reaction plus attachment rate constant" was written as the product of an Arrhenius term and the fluid (or precursor) residence time near the surface in accordance with the "sticking probability" theories of Epstein (1981) and Paterson and Fryer (1988). Epstein assumed that the greater the residence time, the greater would be the opportunity for the chemical reaction to promote attachment, that is, to overcome the hydrodynamic forces which resist attachment. This aspect is quite important since the residence time at the heated surface depends strongly on the fluid mechanics and hence on the geometric design of the fouling test section.

The relationship between initial fouling rate,  $dR_f/dt$ , deposition flux,  $\phi$ , stoichiometric factor,  $m$ , foulant density,  $\rho_f$ , and foulant thermal conductivity,  $k_f$ , was given as follows (Epstein, 1994):

$$\left. \frac{dR_f}{dt} \right|_{t=0} = \frac{m\phi}{k_f \rho_f} \quad (4)$$

The driving force for the mass transfer from the bulk fluid to the reaction surface of a foulant precursor was expressed as the difference between its bulk and surface concentrations,  $c_b$  and  $c_s$ , respectively. The deposition mass flux could ultimately be obtained from Eq. (5) in which  $k'$  and  $k''$  are constants,  $Sc$  is the fluid Schmidt number,  $j_f$  is the friction factor,  $\rho$  is the fluid density,  $\mu$  is the fluid viscosity and  $n$  is the overall order of the reaction plus attachment process.

$$\phi = \frac{c_b}{\left( \frac{k'Sc^{2/3}}{u(j_f)^{1/2}} \right) + \left( \frac{k''\rho u^2 j_f}{\mu \exp(-E/RT_{so})} c_s^{n-1} \right)} \quad (5)$$

The first term in the denominator represents the mass transfer of foulant and/or its precursors to the heated surface. The second term in the denominator represents the reaction and attachment aspects of the fouling process. The reaction part is described by an  $n$ th order process with a true activation energy of  $E$ . The model uses the surface temperature rather than the film temperature. Equation (5) shows that the deposition flux, and hence the fouling rate, has a complex dependence on velocity. Indeed, for all surface temperatures the equation shows that there would be a maximum in the fouling rate-velocity curve. Whilst Epstein was able to use this equation to successfully fit the styrene polymerization fouling data, his model has yet to be tested with the Maya crude oil fouling data because this latter system is far more ill-defined in terms of its physico-chemical properties. As an example, the order of the reaction + attachment term,  $n$ , is unknown for the Maya crude oil fouling but is equal to 5/2 for styrene polymerization.  $Sc$  is unknown for the Maya crude oil but it was possible to make estimates for the styrene polymerization system (Crittenden et al., 1987b). Nonetheless, the form of Eq. (5) provides the same complex dependency of deposition flux on velocity as is seen with the Maya crude oil data (Figs. 3-5). For reaction + attachment control in the absence of mass transfer, *ie* at relatively high velocity and/or at relatively low surface temperature, Eq. (5) would, assuming constant values for  $c_b$ ,  $c_s$  and  $j_f$ , simplify to Eq. (6).

$$\left. \frac{dR_f}{dt} \right|_{t=0} = \frac{k \exp(-E/RT_{so})}{u^2} \quad (6)$$

Combining Eqs. (3) and (6) yields Eq. (7) in which  $k$  is a constant which could effectively be considered to be the pre-exponential factor for the reaction process in which the true activation energy is equal to  $E$ .

$$\left. \frac{dR_f}{dt} \right|_{t=0} = A \exp(-E_A/RT_{so}) = \frac{k \exp(-E/RT_{so})}{u^2} \quad (7)$$

It can now be seen from Eq. (7) why, for the case when there is a constant true activation energy for the actual kinetics of the overall process, there can be such a strong dependency of the apparent activation energy,  $E_A$ , on the fluid velocity,  $u$ , particularly at higher values of velocity. This effect can be seen clearly in Figs. 7 and 8 for the quite different systems of Maya crude oil fouling and styrene polymerization, respectively.

Considerable interest has been expressed in recent years in the concept of threshold fouling for crude oils and how this concept can be incorporated into the design of heat exchanger systems subject to fouling. Wilson et. al. (2005)

have discussed the origins and developments in the Ebert and Panchal semi-empirical approach, including incorporation of Epstein's modelling approach by Polley et al. (2002). The right hand side of Eq. (7) takes a form quite similar to the first term of the Ebert and Panchal correlation, although the index on velocity is somewhat different and the film temperature is used rather than the surface temperature. It ought, in principle nonetheless, to be possible to construct threshold fouling models which take into account the possibility that the fouling rate might either increase or decrease with velocity, according to the balance between mass transfer, reaction and attachment effects postulated by Epstein (1994).

### ISOKINETIC TEMPERATURE

The concept of an isokinetic point in crude oil fouling was proposed by Bennett et al. (2007) who found that the Arrhenius plots for four crude oils all crossed at more-or-less the same temperature. At this temperature, the fouling rates for the four crude oils were therefore the same. In the present paper, the isokinetic concept is developed to take on a different meaning for the case of fouling in a single chemical system (Maya crude oil or styrene polymerization) rather than for a cluster of similar fluids. The straight lines of Figs. 9 and 10 may be written in the form of Eq. (8) in which  $a$  is the gradient (taking the units of mol/kJ) and  $b$  is the intercept.

$$\ln A = aE_A + b \quad (8)$$

Substituting in Eq. (3) yields:

$$\left. \frac{dR_f}{dt} \right|_{t=0} = \exp \left( E_A \left( a - \frac{1}{RT_{SO}} \right) + b \right) \quad (9)$$

Equation (9) applies for each velocity. For this equation to represent all velocities the term inside the exponential must be a constant and hence must not contain the variable  $E_A$ . Isokinetic fouling, in this case defined to occur when the initial fouling rate is independent of velocity, is likely to have a clean (initial) surface temperature which is given approximately by Eq. (10).

$$T_{SO} = \frac{1}{aR} \quad (10)$$

For the Maya crude oil system,  $a = 0.22$  mol/kJ. Hence, a fouling rate independent of velocity should arise when  $T_{SO} = 547$ K. Figure 5 shows that this independence is roughly the case when  $T_{SO} = 274^\circ\text{C}$ . For the styrene polymerization system,  $a = 0.34$  mol/kJ. Hence, a fouling rate independent of velocity should arise when  $T_{SO} = 354$ K. Fig. 11 confirms

that this independence indeed does arise when  $T_{SO} = 81^\circ\text{C}$ . Figure 11 shows clearly the significance of the isokinetic temperature for the better-defined styrene polymerization system. At clean (initial) surface temperatures in excess of the isokinetic temperature, it is likely that the initial fouling rate will show a significant increase with increasing velocity (or mass velocity). At clean (initial) surface temperatures below the isokinetic temperature, it is likely that the initial fouling rate will show a significant decrease with increasing velocity (or mass velocity). Knowledge of the isokinetic temperature is, accordingly, of great interest to designers and operators.

The explanation of why the isokinetic temperature for the styrene polymerization system is much lower than that for the Maya crude oil fouling system is simple. Styrene polymerizes relatively quickly at relatively low temperatures (Crittenden et al., 1997a, b). Therefore, at elevated temperatures it is the rate at which styrene is transported to the hot surface, rather than the rate of reaction and attachment, which tends to control the overall fouling rate. In contrast, fouling from Maya crude oil is a relatively slow process even at relatively high surface temperatures. Accordingly, fouling by Maya crude oil is more likely to be controlled by the rate of the reaction + attachment mechanism until the surface temperature is relatively high. The isokinetic temperature for Maya crude oil ( $274^\circ\text{C}$ ) is of a magnitude similar to that found in the hotter end of crude oil preheat exchanger trains.

For crude oils less prone to fouling than Maya, the isokinetic temperature would be higher and hence fouling could easily be controlled by use of a high velocity. Thus, for a low asphaltene content crude oil such as Australian Gippsland, the isokinetic temperature could be high, leading to the result that an increase in velocity reduces the fouling rate in an annular test apparatus (Saleh et al., 2005). On the other hand, more difficult crude oils are expected to have lower isokinetic temperatures and hence fouling rates could be increased by increasing the tube-side velocity. More difficult crude oils are not solely those with high asphaltene contents since particulate, gum and oxygen contents, etc, are also important parameters (Watkinson, 2007).

Epstein's mass transfer-reaction-attachment model is not fundamentally consistent with the isokinetic temperature concept because Eq. (5) cannot be simplified to yield an expression for deposition flux which is independent of velocity. Hence, an isokinetic temperature cannot be computed directly from the equation. Equation (5) always reveals a maximum in the rate-velocity relationship although, of course, the actual relationship between rate and velocity is expected to be rather shallow for a surface temperature equal to the isokinetic temperature. Indeed, Figs. 5 and 11 both show that the curves are relatively shallow at the isokinetic temperatures for the Maya crude

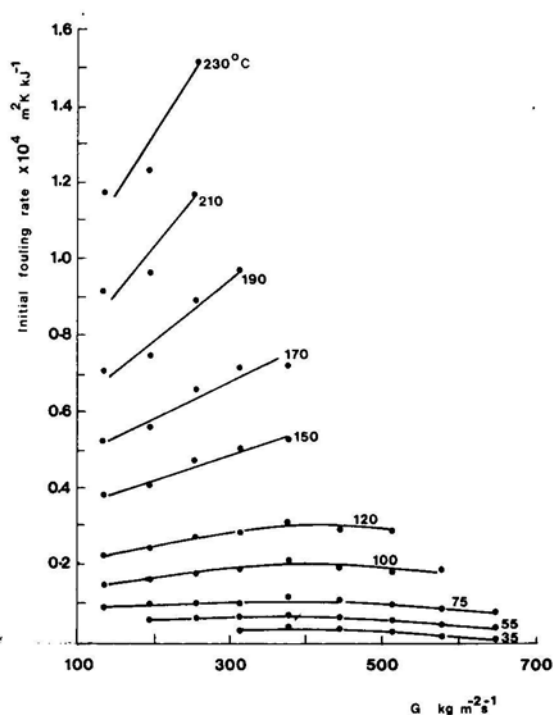


Fig. 11 Initial rates of styrene polymerization fouling (Crittenden et al., 1987a)

oil and styrene polymerization systems, respectively. This is especially the case for the better-defined styrene polymerization system.

## CONCLUSIONS

1. The practical benefits of using a parallel tube test apparatus to obtain initial rate data on the surface fouling at constant heat flux have been demonstrated; the second tube, operated at a constant velocity, is used as a reference.
2. With Maya crude oil, there is a maximum in the initial fouling rate-velocity relationship for each initial (clean) surface temperature in the range 250-280°C. This complex effect of velocity leads to identification of an apparent activation energy for each velocity. Hence, care needs to be exercised when using simple correlative methodologies that include only a single (true) activation energy to guide the design and operation of crude oil preheat exchangers.
3. Strong similarities exist between the Maya crude oil data and earlier data on the polymerization of styrene in odourless kerosene. Both systems show excellent Arrhenius plots for each velocity studied, with values for their apparent activation energies increasing markedly with increasing linear velocity. This strong

velocity effect is consistent with Epstein's mass transfer-reaction-attachment model developed for the styrene system. It is speculated that Epstein's model for initial chemical reaction fouling could be applied to the Maya crude oil system; testing of this speculation is currently underway, although difficulties arise from the ill-defined nature of the Maya crude oil fouling mechanism.

4. The Maya crude oil and styrene polymerization systems both show that the natural logarithm of the pre-exponential factor in the Arrhenius expression depends linearly on the apparent activation energy, leading to identification of a unique isokinetic temperature for each system at which the initial rate of fouling is more-or-less independent of velocity, and is lower for fluids more prone to fouling. For surface temperatures above the isokinetic temperature, the fouling rate might be expected to increase with increasing velocity. The opposite velocity effect arises for surface temperatures lower than the isokinetic temperature.

## ACKNOWLEDGEMENTS

The authors are grateful to Chris Bennett of HTRI for stimulating this comparison of the Maya crude oil and styrene polymerization systems, particularly in terms of their isokinetic temperatures. The authors are grateful also to Asahi Chemical Co. for sponsoring the PhD programme of TT, to EPSRC and BP for sponsoring the PhD programme of DZP, and to Cal-Gavin Ltd. for their support in developing the parallel tube test apparatus. Finally, the wisdom of Norman Epstein in helping to unravel the complexities involved in chemical reaction fouling has been highly valued by the authors.

## NOMENCLATURE

- a* gradient of linear plots of Figs. 9 and 10, mol/kJ  
*A* pre-exponential factor in Arrhenius equation, m<sup>2</sup>K/W  
*b* intercept of linear plots of Figs. 9 and 10  
*c<sub>b</sub>* bulk concentration, kg/m<sup>3</sup>  
*c<sub>s</sub>* surface concentration, kg/m<sup>3</sup>  
*E* true activation energy, kJ/mol  
*E<sub>A</sub>* apparent activation energy, kJ/mol  
*j<sub>f</sub>* friction factor  
*k* pre-exponential factor in Eq. (6)  
*k'* parameter in Eq. (5), m/s  
*k''* parameter in Eq. (5), units depend on value of *n*  
*k<sub>f</sub>* thermal conductivity of foulant, W/mK  
*m* stoichiometric factor in Eq. (4)  
*n* chemical order of fouling reaction  
*q* heat flux, kW/m<sup>2</sup>  
*R* gas constant, kJ/molK  
*R<sub>f</sub>* fouling resistance, m<sup>2</sup>K/W  
*Sc* Schmidt number

$T_b$	bulk temperature, K
$T_s$	surface temperature, K
$T_{so}$	initial (clean) surface temperature, K
$T_{st}$	surface temperature at time t, K
$t$	time, h
$u$	velocity, m/s
$\phi$	deposition mass flux, kg/m <sup>2</sup> h
$\rho$	density of fluid, kg/m <sup>3</sup>
$\rho_f$	density of foulant, kg/m <sup>3</sup>
$\mu$	viscosity of fluid, Pa s

## REFERENCES

- Bennett, C. A., Appleyard, S., Gough, M., Hohmann, R.P., Himanshu, Joshi, H.M., King, D.C., Lam, T.Y., Rudy, T.M. and Stomierowski, S.E., 2006, Industry-recommended procedures for experimental crude oil fouling research, *Heat Transfer Engineering*, Vol. 27 (9), pp. 28-35.
- Bennett, C. A., Kistler, R. S., Nangier, K., Al-Ghawas, W., Al-Hajji, N. and Al-Jemaz, A., 2007, Observation of an isokinetic temperature and compensation effect for high temperature crude oil fouling, *Paper presented at 7<sup>th</sup> International Conference on Heat Exchanger Fouling and Cleaning*, Engineering Conferences International, Tomar, Portugal.
- Crittenden, B.D. and Kolaczkowski, S.T., 1979, Mass transfer and chemical kinetics in hydrocarbon fouling, *Proc. Conference on Fouling Science or Art?, Guildford*, Institution of Corrosion Science and Technology & Institution of Chemical Engineers, London, pp. 169-187.
- Crittenden, B. D. and Khater, E. M. H., 1987, Fouling from vaporising kerosene, *Trans ASME J Heat Transfer*, Vol. 109, pp. 583-589.
- Crittenden, B.D., Hout, S.A. and Alderman, N.J., 1987a, Model experiments of chemical reaction fouling, *Trans IChemE Part A*, Vol. 65, pp. 165-170.
- Crittenden, B.D., Kolaczkowski, S.T. and Hout, S.A., 1987b, Modelling hydrocarbon fouling, *Trans IChemE Part A*, Vol. 65, pp. 171-179.
- Crittenden B. D., Kolaczkowski, S. T. and Takemoto T., 1993, Use of in-tube inserts to reduce fouling from crude oils, *AIChE Symp Series*, Vol. 89 (No. 295), pp. 300-307.
- Energy Institute, 2004, HM40 Guidelines for the Crude Oil Washing of Ships' Tanks and the Heating of Crude Oil being Transported to Sea, Energy Institute, London, p 58.
- Epstein, N., 1981, Fouling: technical aspects, *Fouling of Heat Exchange Equipment*, ed., Somerscales, E.F.C. and Knudsen, J.G., Hemisphere, New York, pp. 31-53.
- Epstein, N., 1994, A model of the initial chemical reaction fouling rate for flow within a heated tube and its verification, *Proc 10<sup>th</sup> International Heat Transfer Conference*, Institution of Chemical Engineers, Rugby, Vol. 4, pp. 225-229.
- Paterson, W.R. and Fryer, P.J., 1988, A reaction engineering approach to the analysis of fouling, *Chemical Engineering Science*, Vol. 43, pp. 1714-1717.
- Phillips, D.Z., 1999, Mitigation of crude oil fouling by the use of HiTRAN inserts, PhD Thesis, University of Bath.
- Polley, G.T., Wilson, D.I., Yeap, B.L. and Pugh, S.J., 2002, Evaluation of laboratory crude oil fouling data for application to refinery pre-heat trains, *Applied Thermal Eng.*, Vol. 22, pp. 777-788.
- Saleh, Z. S., Sheikholeslami, R. and Watkinson, A. P., 2005, Fouling characteristics of a light Australian crude oil, *Heat Transfer Engineering*, Vol. 26, pp. 15-22.
- Tanaka, R., Winans, R.E., Hunt, J.E, Thiyagarajan, P., Sato, S. and Takanohashi, T., 2001, Aggregation of petroleum asphaltene in three different crude oils, *Fuel Chemistry Division Preprints*, Vol. 46(1).
- Takemoto, T., 1993, Use of HiTRAN inserts to reduce fouling from crude oils, PhD Thesis, University of Bath.
- Takemoto, T., Crittenden, B. D. and Kolaczkowski, S. T., 1999, Interpretation of fouling data in industrial shell and tube heat exchangers, *Trans IChemE Part A*, Vol. 77, pp. 769-778.
- Watkinson, A. P., 2007, Deposition from crude oils in heat exchangers, *Heat Transfer Engineering*, Vol. 28, pp. 177-184.
- Wilson, D.I., Polley, G.T. and Pugh, S.J., 2005, Ten years of Ebert, Panchal and the "threshold fouling" concept, *Proc. 6<sup>th</sup> International Conference on Heat Exchanger Fouling and Cleaning: Challenges and Opportunities*, Editors Hans Müller-Steinhagen, M. Reza Malayeri and A. Paul Watkinson, Engineering Conferences International, Klostet Irsee, Germany, pp. 25-36.
- Wilson, E.E., 1915, A basis for rational design of heat transfer apparatus, *Trans ASME*, Vol. 37, pp. 47-89.